rate and practically efficient as applied to many computer graphics and image-processing-related operations. The purpose of our study is to introduce these innovative coordinate systems to a wider audience, thus facilitating their use. In our opinion, the $*I^3$ and $*I^4$ coordinate systems will be useful in many areas of scientific and engineering endeavors.

The author thanks Mr Greg Ferrar for putting his *HyperCuber*2.0 program in the public domain. The drawing of Fig. 2 would have been difficult without this marvelous software. The author is also indebted to Mr Frederick J. Bailey Jr for his kind assistance in proofreading the manuscript.

References

BANCHOFF, T. F. & STRAUSS, C. M. (1978). *The Hypercube, Projections and Slicing*. Chicago: International Film Bureau.
BELL, S. B. M., HOLROYD, F. C. & MASON, D. C. (1989). *Image Vision Comput.* **7**, 194–204.
HER, I. (1993). *ASME J. Mech. Des.* **115**, 447–449.
HER, I. (1995). *IEEE Trans. Image Process.* In preparation.
HER, I. & YUAN, C.-T. (1994). CVGIP: *Graph. Models Image Process.* **56**, 336–347.
KALPAKJIAN, S. (1989). *Manufacturing Engineering and Technology*. Reading, MA: Addison-Wesley.
MERSEREAU, R. M. (1979). *Proc. IEEE*, **67**, 930–949.

Acta Cryst. (1995). A**51**, 662–667

The Wavelength Dependence of Extinction in a Real Crystal: γ-ray Diffraction from NiF_2

BY A. PALMER AND W. JAUCH

Hahn-Meitner-Institut, Glienicker Strasse 100, 14109 *Berlin, Germany*

(*Received* 17 *November* 1994; *accepted* 23 *January* 1995)

Dedicated to Professor W. Prandl on the occasion of his 60th birthday

Abstract

The wavelength dependence of extinction in an NiF_2 crystal of well known mosaicity has been examined by γ-radiation of wavelengths 0.0205, 0.0265, 0.0392 and 0.0603 Å. The results for seven strong low-order reflections, some of them symmetrically equivalent, are related to the extinction models of Becker & Coppens [*Acta Cryst.* (1975), A**31**, 417–425] and Sabine [*International Tables for Crystallography* (1992), Vol. C, pp. 530–533. Dordrecht: Kluwer]. In the considered wavelength region, the extinction-affected observed intensity is approximately a linear function of λ^2, and secondary extinction is found to be dominant. Allowance for pure secondary extinction according to the Becker & Coppens formalism yields both a satisfactory description of the wavelength dependence and mosaicities close to the directly observed ones. With the Sabine model, the influence of the mosaic distribution has to be excluded in order to describe the data properly. Hypothetical assumption of pure primary extinction, however, leads to nonrealistic mosaic-block sizes between 50 and 100 μm. This model is therefore not supported by experiment.

Introduction

Darwin's simple concept of the mosaic crystal and his energy-transport equations form the basis of standard extinction models, which all assume a clear-cut separation into two different extinction mechanisms. The intensity loss associated with coherent scattering in an individual perfect crystal block is termed primary extinction; the loss due to incoherent scattering from several different mosaic blocks is termed secondary extinction.

The theory of Zachariasen (1967) and its development by Becker & Coppens (1974, 1975) has been applied successfully in calculating structure factors close to the observed ones, even though it has some basic deficiencies. In particular, the Darwin equations involve intensities rather than amplitudes and thus the phase-dependent scattering in the case of primary extinction is not treated adequately (*e.g.* Lawrence, 1977).

Within the framework of intensity coupling, Sabine (1992) has proposed a theory in which primary and secondary extinction are treated in a unified way. His formulation, however, leads to an extinction correction factor that shows a substantially different dependence on physical quantities, especially on the wavelength, as compared to the previous theories. It has been included in Volume C of *International Tables for Crystallography* (Sabine, 1992), whereas descriptions of the widely adopted treatments of Zachariasen and Becker & Coppens are missing. It must be emphasized that the reliability of the wavelength variation of extinction corrections is of particular importance in white-beam diffraction techniques, which are used at synchrotron and pulsed spallation neutron sources.

γ-ray diffraction is well suited for an experimental test of different extinction models. Four wavelengths of

an ^{192}Ir source cover a range from 0.0205 to 0.0603 Å and, in a double-crystal mode, an extremely high angular resolution allows for a direct mapping of the mosaic distribution of the sample. Bragg intensities measured at various wavelengths may be used to obtain kinematical structure factors by extrapolation to $\lambda = 0$, regardless of the detailed nature of the extinction process. A requirement for this procedure is data in a region of sufficiently short wavelengths, which is accessible neither by X-rays nor by neutrons.

The purpose of this study is to investigate the wavelength dependence of extinction in a real crystal by experiment, both for its own sake and to test the validity of the different theories. Particular attention is paid to the meaningfulness of the physical parameters that describe the degree of crystal perfection. After an outline of the experimental details and of the considered theoretical models, results for seven strong low-order reflections of NiF_2 are discussed.

Experimental

The γ-ray diffractometer at the Hahn-Meitner-Institut is equipped with an ^{192}Ir source radiating at 0.0205, 0.0265, 0.0392 and 0.0603 Å. The dimensions of the NiF_2 single-crystal sample were 1.5 mm along [110], 3.3 mm along [$\bar{1}$10] and 2.8 mm along [001]. The tetragonal cell parameters are $a = 4.6501$ and $c = 3.0835$ Å.

Intrinsic reflection profiles have been recorded by high-resolution γ-ray diffraction, where the sample is exposed to a Bragg reflection from a highly perfect Si crystal with an angular width of about 1.5″. Gaussian distributions have been fitted to the profiles of the different reflections, resulting in full widths at half-maximum (FWHM) between 16 and 25″. The examples in Fig. 1 show that the assumed Gaussian shapes do not perfectly describe the real mosaicity. The widths of these distributions, however, are adequate measures of the crystal perfection.

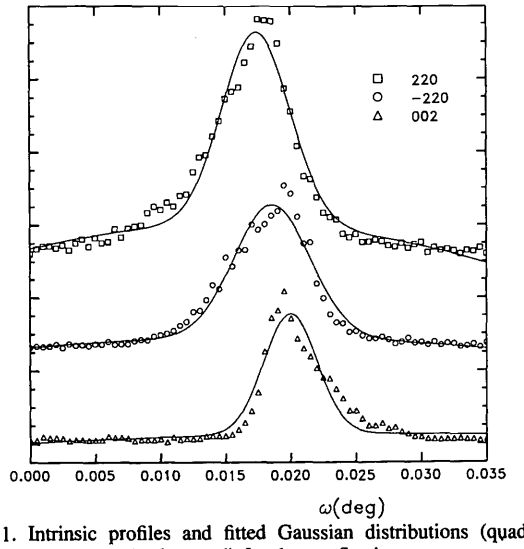

Fig. 1. Intrinsic profiles and fitted Gaussian distributions (quadratic background) for three reflections.

Each wavelength was selected by means of a single-channel analyzer with a window of a few keV. The relative intensities of the four γ lines in order of increasing wavelength are 11/60/100/3.8. Owing to the smaller scattering power at shorter wavelengths, most of the measurement time had to be spent at $\lambda = 0.0205$ Å, where a counting-statistical precision of 1% for a strong reflection required about 15 h with a source activity of 80 Ci (1 Ci = 3.7×10^{10} Bq).

The absorption coefficient μ as calculated from the scattering cross sections given by Hubbel (1982) varies from 0.37 cm^{-1} at $\lambda = 0.0205$ Å to 0.58 cm^{-1} at $\lambda = 0.0603$ Å. Absorption factors and mean path lengths $\bar{T}$ have been obtained by the analytical algorithm implemented in *XTAL* (Hall & Stewart, 1989).

For scaling the intensities, four high-order reflections ($\sin\theta/\lambda = 0.56 - 0.92$ Å^{-1}) of intermediate intensity have been measured to about 1% counting-statistical precision. Their absolute values are known from the results of a structure refinement based on an extended data set of 298 independent reflections at $\lambda = 0.0392$ Å (Palmer & Jauch, 1993). The fact that the weak extinction in these reflections is less than 1% has been taken into account. The random errors of the strong reflections are dominated by the uncertainty in the scale factors. At the shorter wavelengths, the inner reflections suffer from a large background owing to their low Bragg angles down to $\theta = 0.18°$. For this reason, the innermost reflections 110 and $\bar{1}$10 could not be measured with adequate accuracy and have not been included in the detailed analysis. The scaled values of $|F_{obs}|^2$ at the four different wavelengths are listed in Table 1.

Extinction models

We now briefly outline the relevant extinction formulae by Becker & Coppens and by Sabine. For details on their foundations, the reader is referred to the original articles.

In 1967, Zachariasen proposed a simple and practically successful model of extinction. Even though it contains a number of shortcomings, in least-squares refinements it often yields satisfactory agreement between observed and calculated structure amplitudes. A considerable improvement was made by Becker & Coppens (1974), who took into account the angular dependence of the particle-size effect and allowed for a Lorentzian distribution of the mosaic-block orientation. For the sake of simplicity, however, we will restrict our discussion to Gaussian distributions.

The extinction factor is defined as $y = I_{obs}/I_{kin}$, where I_{obs} is the observed integrated intensity and the kinematic intensity I_{kin} is proportional to

$$Q = (F^2/V^2)(\lambda^3/\sin 2\theta)$$

Table 1. *Scaled values of $|F_{obs}|^2$ and their associated standard deviations at the four different wavelengths*

λ (Å)	220	$\bar{2}20$	330	$\bar{3}30$	211	002	301
0.0205	2167 (22)	2019 (20)	1100 (19)	1046 (20)	1702 (17)	2317 (23)	1896 (19)
0.0265	2107 (21)	1918 (19)	1080 (11)	1033 (10)	1652 (17)	2218 (22)	1810 (18)
0.0392	2003 (20)	1718 (17)	1086 (11)	1003 (10)	1582 (16)	1922 (19)	1681 (17)
0.0603	1910 (19)	1431 (14)	1029 (10)	896 (9)	1405 (14)	1468 (15)	1372 (14)

with F being the modulus of the structure factor in units of scattering length and V the unit-cell volume. Note that the polarization factor is close to unity because of the small diffraction angles for γ-rays. The microstructure of the crystal is characterized by a mosaic-spread parameter, g, and the path length in a perfect domain, t. For a Gaussian mosaic distribution of FWHM δ, $g = (2\ln 2/\pi)^{1/2}/\delta$.

Becker & Coppens (1974, 1975)

The extinction coefficient is factorized into expressions for primary and secondary extinction:

$$y = y_p(x_p)y_s(y_p x_s)$$

with

$$x_p = \tfrac{2}{3}Qt(t\sin 2\theta/\lambda) \qquad (BC.35)$$

and

$$x_s = \tfrac{2}{3}Q\bar{T}\{[\lambda/(t\sin 2\theta)]^2 + [1/(2g^2)]\}^{-1/2}. \quad (BC.40b)$$

Each term has the form

$$y_i = \{1 + C_i x_i + A_i(\theta)x_i^2/[1+B_i(\theta)x_i]\}^{-1/2}, \quad i = p, s, \qquad (BC.37)$$

where $C_p = 2$ and $C_s = 2.12$. $A_i(\theta)$ and $B_i(\theta)$ as given in (*BC*.38) and (*BC*.43) are valid for weakly absorbing crystals with $\bar{T}_{max}/\bar{T}_{min} < 2$. This model will be referred to as BC.

For pure secondary extinction ($y_p = 1$), the useful limiting cases of type-I (mosaic-spread) and type-II (particle-size) broadening of the reflection curve will be referred to as BC-I and BC-II. Thus,

$$x_I = (2 \times 2^{1/2}/3)g\bar{Q}\bar{T}$$

and

$$x_{II} = \tfrac{2}{3}(t\sin 2\theta/\lambda)\bar{Q}\bar{T},$$

respectively. Zachariasen's expression for type-I extinction (ZACH-I) has the simple form $y_s = (1+2g\bar{Q}\bar{T})^{-1/2}$, which represents a first-order approximation to BC-I.

Sabine (1992)

In an intuitively obvious way, this approach relates two angular distributions, the mosaicity of the sample and the Darwin width of a reflection. Primary and secondary extinction are then no longer separable:

$$x = [(\lambda F/V)t + gQ(\bar{T} - t)]^2. \qquad (S.6.4.8.2)$$

The angular dependence of the extinction factor is approximated by a weighted average of the values derived for $2\theta = 0$ and π. For small Bragg angles and weak absorption effects as in γ-ray diffraction, the extinction factor reduces to

$$y = 1 - x/2 + x^2/4 - 5x^3/48 + 7x^4/192, \quad x \le 1; \qquad (S.6.4.5.1)$$

$$y = (2/\pi x)^{1/2}[1 - 1/(8x) - 3/(128x^2) - 15/(1024x^3)], \quad x > 1. \qquad (S.6.4.5.2)$$

The series truncation gives rise to a small discontinuity at $x = 1$ which can be tolerated in practice.

Limiting cases here are not type-I or type-II crystals but only pure primary or secondary extinction:

$$x_p = [(\lambda F/V)t]^2 \quad \text{and} \quad x_s = (g\bar{Q}\bar{T})^2.$$

The general expression and the two limiting cases of the Sabine model will be abbreviated as SAB, SAB-P and SAB-S, respectively. We have used actual values of $\bar{T}$ for individual reflections instead of the crystal size in the original work.

As illustrated in Fig. 2, the two models predict quite different dependencies of y on wavelength and block size. BC yields $y = 1$ for the zero interaction limits, $\lambda = 0$ and $t = 0$, whereas SAB does not for the latter case. For a given mosaic spread, the actual wavelength dependence of a reflection will be described by different block sizes for the two models. According to Sabine's model, a single perfect crystal results in the limit of the mosaic spread reaching zero, whereas the other theories assume parallel blocks that are uncorrelated, *i.e.* separated by random displacements.

Results

The above models have been fitted to the measured intensities using the program *MINUIT* (James & Roos, 1975). Two parameters have been varied, the kinematical structure-factor amplitude $F(\lambda = 0)$ and, for BC, BC-II, SAB and SAB-P, the block size t; the terms containing g have been calculated from the observed

Table 2. *Results from fitting the different extinction models to the experimental intensities*

The e.s.d.'s (in parentheses) have not been multiplied by the goodness-of-fit parameter.

$$\chi^2 = \sum (F^2_{obs} - F^2_{calc})^2 / \sigma^2_{obs}.$$

		220	$\bar{2}20$	330	$\bar{3}30$	211	002	301
	$\bar{T}$ (cm)	0.145	0.327	0.145	0.325	0.145	0.158	0.174
	δ_{obs} ($''$)	23	22	23	22	20	16	18
BC	F^2 ($\lambda = 0$)	2170 (18)	2099 (19)	1104 (11)	1077 (11)	1739 (15)	2519 (25)	1985 (18)
	t (μm)	1.4 (3)	13 (7)	7 (2)	30 (7)	24 (5)	60 (2)	50 (2)
	χ^2	7.4	6.0	2.4	1.2	0.8	0.4	1.6
BC-I	F^2 ($\lambda = 0$)	2170 (18)	2099 (19)	1105 (11)	1077 (11)	1739 (15)	2504 (23)	1981 (17)
	δ ($''$)	32 (4)	21.5 (9)	22 (5)	17 (2)	16 (1)	7.9 (2)	9.8 (4)
	χ^2	7.4	6.0	2.4	1.2	0.8	0.6	1.4
BC-II	F^2 ($\lambda = 0$)	2170 (18)	2099 (19)	1105 (11)	1077 (11)	1739 (15)	2504 (23)	1981 (17)
	t (μm)	1.0 (1)	1.49 (6)	0.9 (2)	1.2 (1)	2.0 (1)	3.8 (1)	2.7 (1)
	χ^2	7.4	6.0	2.4	1.2	0.8	0.6	1.4
SAB	F^2 ($\lambda = 0$)	2143 (17)	2024 (19)	1101 (10)	1064 (10)	1715 (14)	2433 (23)	1946 (18)
	t (μm)	27 (3)	46 (2)	35 (5)	55 (3)	46 (2)	70 (2)	64 (2)
	χ^2	12	20	2.0	0.6	1.8	3.4	2.0
SAB-P	F^2 ($\lambda = 0$)	2171 (18)	2104 (12)	1105 (11)	1078 (8)	1741 (15)	2539 (31)	1994 (20)
	t (μm)	46 (3)	86 (2)	44 (5)	76 (4)	65 (2)	97 (2)	86 (2)
	χ^2	7.2	3.8	2.4	1.4	0.8	0.6	2.2
SAB-S	F^2 ($\lambda = 0$)	2112 (13)	1940 (13)	1091 (8)	1037 (8)	1671 (15)	2247 (15)	1846 (12)
	δ($''$)	9.4 (6)	10.5 (2)	4.5 (5)	5.8 (3)	5.9 (2)	4.6 (1)	4.6 (1)
	χ^2	19	54	1.2	0.6	9.0	54	20
ZACH-I	F^2 ($\lambda = 0$)	2176 (19)	2148 (23)	1105 (11)	1081 (12)	1749 (16)	2641 (31)	2016 (21)
	δ ($''$)	28 (3)	16.1 (8)	22 (5)	15 (2)	14 (1)	5.3 (2)	7.6 (4)
	χ^2	6.6	1.4	2.4	1.8	0.8	4.0	3.0

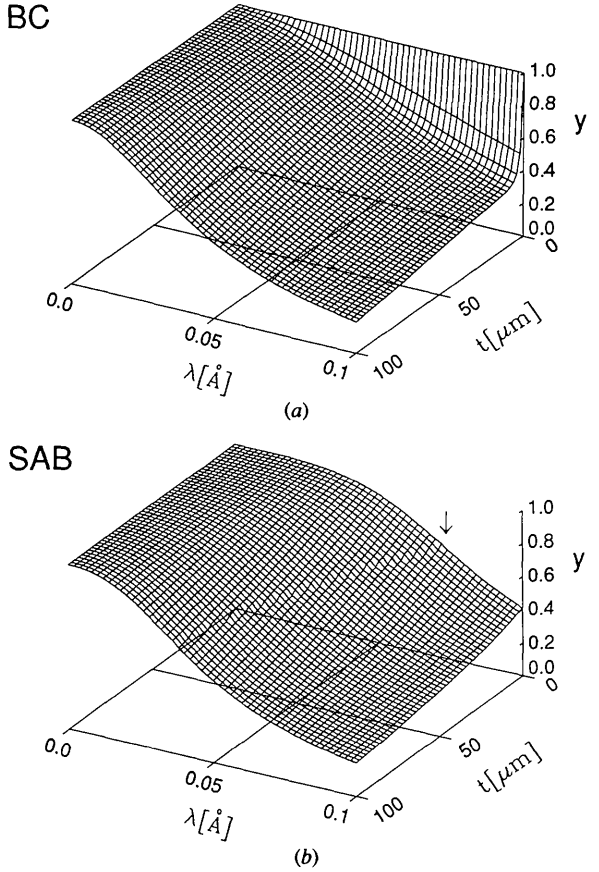

Fig. 2. Extinction coefficients as functions of wavelength and mosaic-block size for the two different general models (*a*) BC and (*b*) SAB. Values are calculated for $F = 50 r_e$ ($r_e = 2.82$ fm), $\sin\theta/\lambda = 0.15$ Å^{-1}, $\delta = 17''$ and $\bar{T} = 0.16$ cm. In the case of SAB, the arrow marks the discontinuity in $y(x)$.

mosaic distributions. In the cases of BC-I and SAB-S, the Gaussian FWHM δ was the second parameter. Simultaneous variation of both t and δ suffers from almost complete correlations (≥ 0.99).

The results are summarized in Table 2. As we are dealing with only two degrees of freedom, the sensitivity of statistical figures of merit is limited. Roughly, the critical value of χ^2 at the 5% level (= 6.0) confines a reasonable boundary for a fit to be statistically acceptable. One should bear in mind that the e.s.d.'s of the parameters are meaningful quantities only to the extent that a model properly describes the data. Most of the fits are displayed in Figs. 3–5, where F^2 is plotted against λ^2, since for small Bragg angles and moderate extinction the wavelength dependence may be approximated by

$$y(\lambda) = 1 - k\lambda^2.$$

Extrapolations from symmetry-equivalent reflections should lead to identical structure factors in the kinematic limit, $\lambda = 0$, thus providing a strong criterion for an assessment of the fits.

In Fig. 3, different slopes are found for symmetry-equivalent reflections with different mean path lengths through the crystal. The same holds for the pair 330 and $\bar{3}30$, and for the 110 and $\bar{1}10$ reflections. There is thus unambiguous evidence for the presence of secondary extinction, primary extinction being independent of the path length.

In Figs. 3–5, the SAB-S curves approach $\lambda = 0$ with zero slope and show poor agreement with the data (except for 330 where extinction is weak). SAB-P fits the data much better, even better than does SAB (see also Table 1). Results for BC-I are not shown

in the figures since they are indistinguishable from BC-II. All the BC models fit the data equally well, yielding virtually identical kinematic structure factors. The calculated primary-extinction coefficients y_p (for the BC general case) are close to unity. Exceptions are the 002 and 301 reflections where large calculated t values bring y_p to about the same magnitude as y_s.

To obtain information on the path-length dependence of the 002 intensity, in a further experiment at $\lambda = 0.0392$ Å, diffraction data were recorded at various ψ settings around the scattering vector. Fig. 6 shows that the intensity variation is rather small even though $\bar{T}$ varies by more than a factor of 2. However, this does not validate any predominance of primary extinction since the mosaic spread was observed to increase roughly proportional to $\bar{T}$. Therefore, the extinction factors calculated from BC-I (and ZACH-I) are nearly independent of $\bar{T}$. Application of SAB-S yields extinction factors close to unity but, as is obvious from Fig. 5, y is considerably smaller at 0.0392 Å.

The type-I models for which δ is an adjustable parameter produce values for the mosaicity that come close to the direct observations. For the 002 and 301 reflections, however, the degree of perfection appears to be too high, a feature that also occurs with the general models where the resulting block sizes are unusually large.

Structure factors and quality of fit for SAB-P and BC-II almost coincide as a consequence of the similar wavelength dependence in these models. However, the

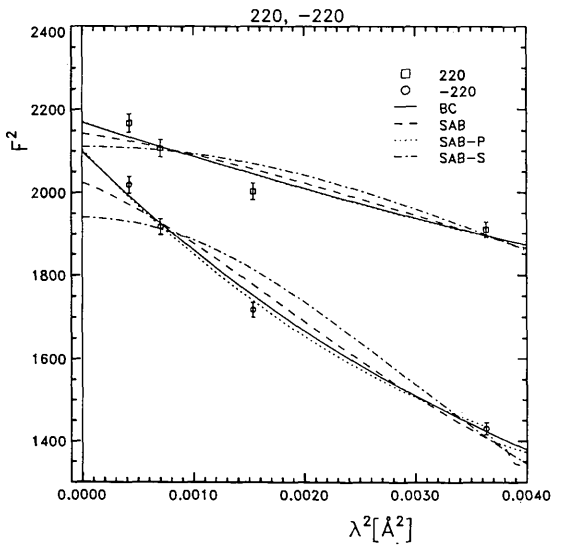

Fig. 3. Squared structure factors of the 220 and $\bar{2}20$ reflections and calculated wavelength dependencies from indicated models.

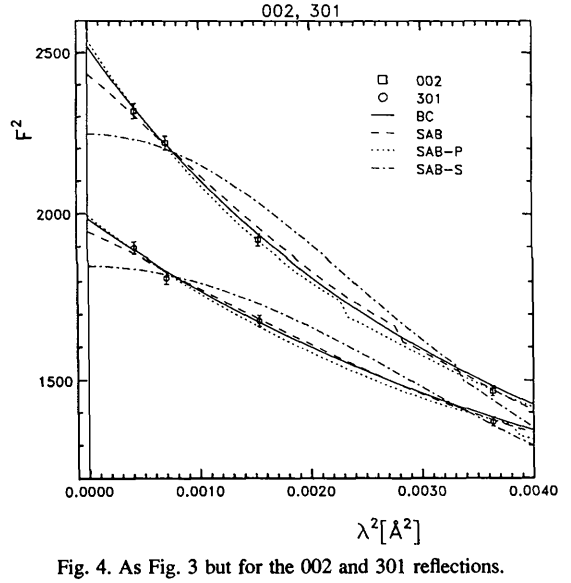

Fig. 4. As Fig. 3 but for the 002 and 301 reflections.

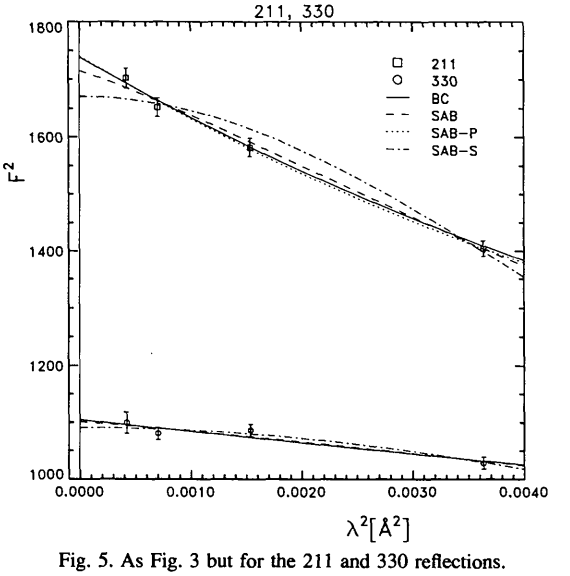

Fig. 5. As Fig. 3 but for the 211 and 330 reflections.

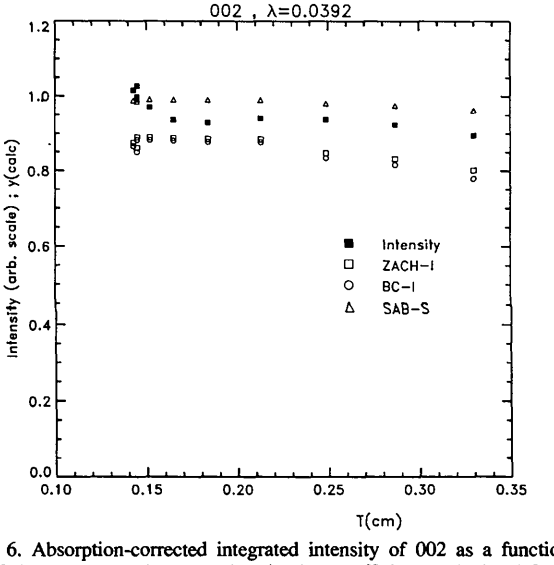

Fig. 6. Absorption-corrected integrated intensity of 002 as a function of the mean path length and extinction coefficients calculated from models of secondary extinction with the observed variation of the mosaicity taken into account.

results for the block sizes are very different. BC-II yields realistic values of a few μm, whereas SAB-P gives block sizes almost as large as typical sample sizes in X-ray experiments.

Discussion

Using the Sabine model, one has to exclude any effect of the mosaic distribution, otherwise the observed wavelength dependence is improperly described. Tentative assumption of pure primary extinction yields extremely large block-size values, which have to be compared with the extinction length

$$t_{ext} = V/(F\lambda).$$

t_{ext} marks a limit for the applicability of kinematic theory: $t \leq t_{ext}$. With respect to γ-radiation between 0.06 and 0.02 Å, t_{ext} varies from 80 to 240 μm for the 002 reflection. The mosaic-block dimensions from SAB-P are of the same order of magnitude. For such a large block size, no secondary extinction could be present as there were not enough blocks diffracting simultaneously in the sample. On the other hand, it has been shown that secondary extinction is important in the examined crystal.

Allowance for primary extinction in the general Becker & Coppens model leads to highly anisotropic block dimensions, which in the case of the 002 and 301 reflections are very large in size. The degree of anisotropy is doubtful as it is not reflected in the mosaic spreads. Assumption of particle-size-dominated secondary extinction (BC-II), however, yields nearly isotropic values for t, with a much more realistic magnitude. The inconsistency between the BC and BC-II parameters can probably be attributed to the inadequate phenomenological description of primary extinction.

The BC type-I model provides mosaicities that come very close to the observation. It is not possible to distinguish between type I and type II on the basis of statistical indicators: both models lead to equally good fits with physically reasonable parameters and it seems to be immaterial which type comes closer to reality. A preference of the mosaic-spread description may be justified by its direct experimental access. It is noteworthy that for the type-I model, at least in the range of extinction considered ($y > 0.6$), the simple formulation of Zachariasen also leads to reliable results.

The fact that, for the 002 and 301 reflections, the degree of crystal perfection deduced from both type-I and type-II models is higher by roughly a factor of 2, as compared to the other reflections and to the observations, might be related to significant deviations of the observed mosaic distributions from Gaussian shapes (Fig. 1 shows an asymmetric triangular profile for 002).

Concluding remarks

Selected integrated intensities from a well characterized single crystal have been measured as a function of path length and of wavelength in the region from 0.02 to 0.06 Å. The dependence of extinction on the experimental control variables allows an assessment of the validity of rival theoretical descriptions.

In the case of the recent model of Sabine, assumption of primary extinction leads to nonrealistic estimates of the mosaic-block size, while the assumption of secondary extinction leads to a bad description of the observed wavelength dependence. The situation is much better with the Becker & Coppens formalism. Here, assumption of coexistence of primary and secondary extinction sometimes yields very large mosaic blocks too, but restriction to pure secondary extinction leads to reasonable block sizes for type II and to mosaic spreads that come close to observation for type I. The latter case is equally well described by the Zachariasen model.

Thus, in structure refinements, the extinction model advocated in Volume C of *International Tables for Crystallography* may provide calculated structure factors close to observed ones but, since it suggests an incorrect nature of the extinction process, it cannot be recommended for use.

References

BECKER, P. J. & COPPENS, P. (1974). *Acta Cryst.* **A30**, 129–147.

BECKER, P. J. & COPPENS, P. (1975). *Acta Cryst.* **A31**, 417–425.

HALL, S. R. & STEWART, J. M. (1989). Editors. *XTAL2.6 Users Manual.* Univs. of Western Australia, Australia, and Maryland, USA.

HUBBEL, J. H. (1982). *Int. J. Appl. Radiat. Isot.* **33**, 1269–1290.

JAMES, F. & ROOS, M. (1975). *Comput. Phys. Commun.* **10**, 343–367.

LAWRENCE, J. L. (1977). *Acta Cryst.* **A33**, 232–234.

PALMER, A. & JAUCH, W. (1993). *Phys. Rev.* **B48**, 10304–10310.

SABINE T. M. (1992). *International Tables for Crystallography*, Vol. C, pp. 530–533. Dordrecht: Kluwer.

ZACHARIASEN, W. H. (1967). *Acta Cryst.* **23**, 558–564.